



ELSEVIER

Computational Materials Science 2 (1994) 319–325

COMPUTATIONAL
MATERIALS
SCIENCE

Influence of variations of temporal pulse shape in excimer laser processing of semiconductors

R. Černý^a, V. Vydra^a, K.M.A. El-Kader^b and V. Cháb^b

^a Department of Physics, Faculty of Civil Engineering, Czech Technical University, Thákurova 7, 166 29 Prague 6, Czech Republic

^b Institute of Physics, Czech Academy of Sciences, Na Slovance 2, 180 40 Prague 8, Czech Republic

(Received 15 October 1993; accepted 8 November 1993)

Abstract

The effects of the time structure of the energy distribution in excimer laser pulse on melting and solidification of Si have been analyzed for pulses with the same FWHM but different tails at the fall time site. The numerical calculations using a nonequilibrium thermal model have shown a strong dependence of the melting threshold E_t and melting time t_m on the ratio of the energies distributed in the main peak and the tail. With decreasing ratio, E_t increases and t_m decreases, which is in a contradiction to the previous calculations, and a shift to the equilibrium conditions at the surface is predicted.

1. Introduction

Experimental investigations of laser effects on materials in early 60's were qualitative due to the poor reproducibility and beam quality. Later, the development of Nd-based lasers in 70's which are inherently more stable and deliver optically superior beams brought a better reproducibility of experiments and this trend continued in using excimer laser in 80's. Although the stability and homogeneity of laser beams have been continuously improved, there are still observed fluctuations in the energy density, the duration time and the pulse shape depending on the working parameters of the laser. These fluctuations are often underestimated.

In most experimental works [1–7] pulse duration using full width at half maximum (FWHM) values is reported without an exactly defined pulse shape and without being considered in fluctua-

tions. Numerical analysis by Wood and Giles [8] for solid-state-laser pulse shapes showed that large variations in the pulse shape from rectangular to Gaussian including various triangular shapes can alter the melt front penetration. Analogous calculation for excimer lasers [9,10] with trapezoidal shape and various pulse durations confirmed the significant influence of the pulse parameters on the time evolution of the molten layer thickness and the value of energy density corresponding to the melting threshold.

These analyses were performed as parametric studies only, with the primary aim to demonstrate how critical the fluctuations in laser pulse are for some phenomena of the annealing process [8].

In this paper, we analyze variations of the energy distribution in the time structure of an excimer laser pulse, XeCl (308 nm), at FWHM approximately constant. Experimentally measured pulse shape rise time and fall time are used

as input parameters in our mathematical model of laser-induced nonequilibrium phase changes of Si(100) [11,12]. The consequences of variations of the pulse parameters for basic characteristics of the laser-induced melting and solidification are calculated.

2. Experimental

In our experiments we used the experimental setup described in Ref. [1]. Samples cut from 0.35 mm thick wafers of the Czochralski-grown, p-type Si(100) single crystals (5–12 Ωcm), were irradiated in a UHV chamber (the basic pressure lower than 10^{-8} Pa) by the XeCl (308 nm) excimer laser LAMBDA LPX 250iC. The pulse shapes were analyzed depending on the working voltage ranging from 16 kV to 24 kV. The energy of the individual pulse was monitored by the Coherent Labmaster pyrometer equipped with the LM-P5 measuring head. The time pulse structure of the excimer laser was detected with a Si-photodiode (rise time < 1 ns). Photodiode signals were amplified by a short-range amplifier (10–100 MHz) and captured by the Phillips PM 3323 oscilloscope and stored in a PC.

Depending on the working voltage, three different pulse structures were found. The characteristic energy distributions in pulses are shown in Fig. 1.

As demonstrated in Fig. 1, the single triangular or trapezoidal shape of the pulse with constant FWHM cannot be considered. For a model application, the real pulses were parametrised. The main parameters used for the pulse characterization are displayed in Fig. 2. The duration of a pulse is divided into the rise time (A), width of the plateau (B), fall time (C), and tail (D). The distribution of the energy density in a pulse is given by the ratio A_1/A_2 , where A_1 is the area of the peak and A_2 the area of the tail. The used parameters of the pulses are summarized in Table 1. The most remarkable differences in laser pulse shape depending on applied voltage are laser pulse duration E and pulse and tail area (i.e. energy density) ratio A_1/A_2 (see Fig. 2). As the "main" pulse duration ($A + B + C$), and conse-

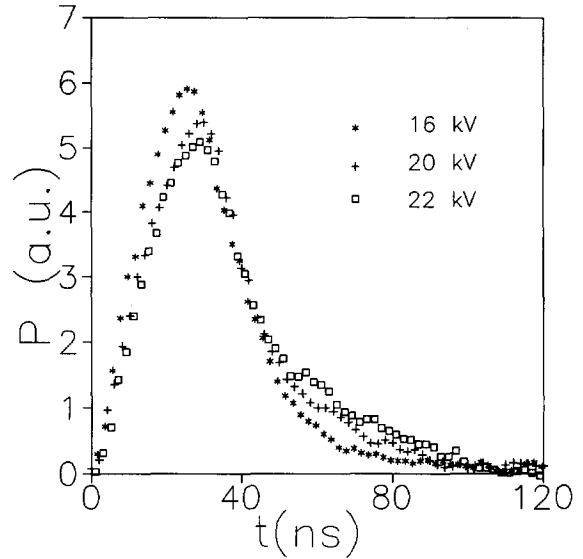


Fig. 1. Temporal pulse shapes of XeCl laser for various applied voltages.

quently, also the FWHM value, varies nonsignificantly, the only important variation of the pulse duration $E = A + B + C + D$ is due to the changes in tail duration (D).

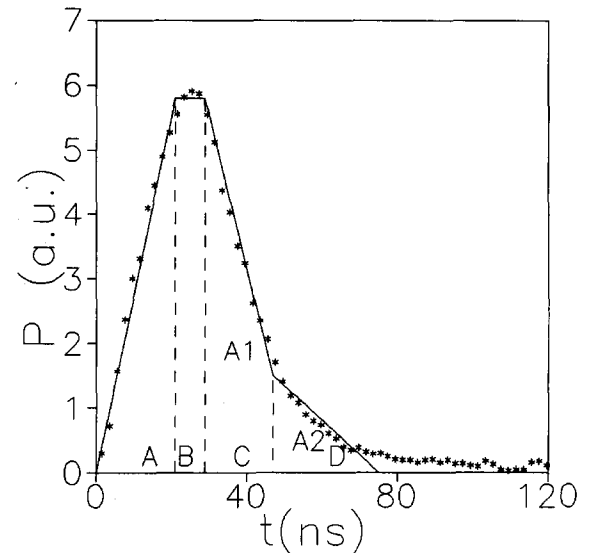


Fig. 2. Approximation of a real pulse for using in numerical analysis.

3. Mathematical model

For the theoretical simulations, the nonequilibrium thermal model of laser induced melting and solidification, which we have developed before (see [11,12] for details), was used:

$$\rho c_i \frac{\partial T}{\partial t} = \frac{\partial}{\partial x} \left(K_i \frac{\partial T}{\partial x} \right) + S(x, t) \quad \text{in } \Omega_i, i = l, s \quad (1)$$

$$\rho L \dot{Z}(t) = K_s \frac{\partial T}{\partial x} \Big|_{x=Z^+} - K_l \frac{\partial T}{\partial x} \Big|_{x=Z^-}, \quad (2)$$

$$\frac{\partial T}{\partial x} \Big|_{x=0^+} = 0, \quad (3)$$

$$T(D, t) = T_0, \quad (4)$$

$$T(x, 0) = T_0, \quad (5)$$

where ρ is the density, c_i is the specific heat, K_i is the thermal conductivity, L is the latent heat, t time, x space variable, $Z(t)$ is the location of the moving boundary between the solid and liquid phases, $\dot{Z}(t) = dZ(t)/dt$, Ω_i is the space subdomain occupied by phase i , $\Omega_l + \Omega_s = \Omega$, $\Omega = \langle 0, D \rangle$. D is the size of the spatial domain (thickness of the sample), indices l and s denote the liquid and the solid, respectively. The source term $S(x, t)$ in the Eq. (1) describes the energy absorption of a laser pulse

$$S(x, t) = (1 - R)\alpha I_0(t) \exp(-\alpha x), \quad (6)$$

where R is the reflectivity, α the optical absorption coefficient, $I_0(t)$ the pulse intensity profile.

The interface response function following from the Jackson–Chalmers theory is chosen to ex-

press the dependence of the interface velocity on its temperature under nonequilibrium thermal conditions:

$$\begin{aligned} \dot{Z}(T_Z) = f(T_Z) = C_1 \exp(-Q/k_B T_Z) \\ \times \left(1 - \exp\left[-L_p \left(\frac{1}{T_Z} - \frac{1}{T_{eq}} \right) / k_B \right] \right). \end{aligned} \quad (7)$$

Here, Q denotes the activation energy for self-diffusion in the liquid, L_p is the latent heat of fusion per particle and C_1 is a material constant. Then the interface temperature T_Z is not equal to T_{eq} , hence the latent heat L in the Stefan condition (2) must depend on T_Z (to assure the conservation of energy):

$$L(T_Z) = L_{eq} + (T_Z - T_{eq})(c_l - c_s), \quad (8)$$

where L_{eq} is the latent heat measured at the equilibrium phase transition temperature T_{eq} .

In the reflectivity calculation, we consider a system of two absorbing media l-Si and c-Si each of them being optically homogeneous in the directions of y, z -axis, and in x -axis being characterised by a continuously changing complex permittivity function $\hat{\epsilon} = \hat{\epsilon}(x)$. The permeabilities μ of l-Si and c-Si are assumed to be constant and equal to the permeability of vacuum μ_0 . Thus, the optical inhomogeneity is involved by temperature dependence of the complex refraction index \hat{n} and by existence of the temperature gradient in x -direction in the sample. The system is assumed to border on two semi-infinite optically homogeneous media by plane interfaces $x = 0$ and $x = D$, the interface between both inhomogeneous media being also a plane $x = Z(t)$.

In the numerical solution, we introduce Landau's transformations

$$\zeta = \frac{x}{Z(t)}, \quad x \in \langle 0, Z(t) \rangle \quad (9)$$

and

$$\xi = \frac{x - Z(t)}{D - Z(t)}, \quad x \in \langle Z(t), D \rangle \quad (10)$$

to convert the subdomains Ω_l, Ω_s into two fixed space intervals Ω'_l, Ω'_s .

Table 1

Influence of the applied voltage on the temporal pulse shape of XeCl laser

U (kV)	A (ns)	B (ns)	C (ns)	D (ns)	E (ns)	A_1/A_2
24	24	10	20	47	101	3.97
22	24	10	21	44	99	3.70
21	23	11	17	42	93	4.84
20	21	9	23	33	86	6.13
19	21	10	25	20	76	11.2
18	21	10	22	20	73	10.0
16	21	8	24	22	75	10.9

Using Eqs. (9) and (10), Eqs. (1) and (2) are transformed into the form:

$$\rho c_l \left(\frac{\partial T}{\partial t} - \dot{Z} \frac{\zeta}{Z} \frac{\partial T}{\partial \zeta} \right) = \frac{1}{Z^2} \frac{\partial}{\partial \zeta} \left(K_l \frac{\partial T}{\partial \zeta} \right) + S(Z, \zeta, t) \quad \text{in } \Omega'_l = \langle 0, 1 \rangle \quad (11)$$

$$\rho c_s \left(\frac{\partial T}{\partial t} - \dot{Z} \frac{1-\xi}{D-Z} \frac{\partial T}{\partial \xi} \right) = \frac{1}{(D-Z)^2} \frac{\partial}{\partial \xi} \left(K_s \frac{\partial T}{\partial \xi} \right) + S(Z, \xi, t) \quad \text{in } \Omega'_s = \langle 0, 1 \rangle \quad (12)$$

$$\rho L_{\text{eq}} \dot{Z}(t) = \frac{1}{D-Z} K_s \frac{\partial T}{\partial \xi} \Big|_{\xi=0^+} - \frac{1}{Z} K_l \frac{\partial T}{\partial \zeta} \Big|_{\zeta=1^-} \quad (13)$$

Then, the standard Galerkin-type finite-element procedure with both space and time discretization results in a set of algebraic equations (see Ref. [11] for details)

$$\bar{H}(Z, \dot{Z}) \{T\}_{t+\Delta t} = \bar{P}(Z, \dot{Z}) \{T\}_t - \{\bar{U}(Z, t)\} - \{B(Z, \dot{Z})\}, \quad (14)$$

where

$$\bar{H}(Z, \dot{Z}) = \frac{2}{3} H(Z, \dot{Z}) + \frac{1}{\Delta t} P(Z), \quad (15)$$

$$\bar{P}(Z, \dot{Z}) = \frac{1}{\Delta t} P(Z) - \frac{1}{3} H(Z, \dot{Z}), \quad (16)$$

$$\{\bar{U}(Z, t)\} = \frac{1}{3} \{U(Z, t)\}_t + \frac{2}{3} \{U(Z, t)\}_{t+\Delta t}, \quad (17)$$

Δt is the length of a time element, $P(Z)$ and $H(Z, \dot{Z})$ are square matrices, column vectors $\{T\}$,

$\{U(Z, t)\}$ and $\{B(Z, \dot{Z})\}$ represent the temperature field, source term and boundary conditions, respectively, $\{T\} = \langle T_{11}, \dots, T_{1,n-1}, T_{s1}, \dots, T_{sm} \rangle^T$, $T_{ln} \equiv T_{s1}$, n is the number of points in the liquid and m is the number of points in the solid.

Conditions (2) and (7) that apply to the moving boundary, are treated in the following way: the Stefan condition (2) is involved in Eq. (14), hence $\{B(Z, \dot{Z})\}$ has the form

$$\{B(Z, \dot{Z})\} = \left(\underbrace{0, \dots, 0}_{n-1}, \rho f(T_Z) [L_{\text{eq}} + (c_s - c_l) T_{\text{eq}}], \underbrace{0, \dots, 0}_{m-1} \right)^T, \quad (18)$$

where $f(T_Z)$ is the interface response function (7), the condition (7) becomes the convergence criterion of the iteration procedure which is designed as a successive approximation approach.

4. Numerical results and discussion

A series of numerical calculations was performed to test the influence of varying pulse duration E and ratio A_1/A_2 using the experimental data as input parameters in the model. In this analysis, Si(100) melting and solidification were studied. The thermodynamic and optical parameters of the crystalline and liquid Si were taken from [10,15–17] being considered as temperature dependent. The initial sample temperature was taken $T_0 = 293$ K.

In the first part of our numerical simulations,

Table 2

Influence of the temporal pulse shape variations on the characteristic parameters of Si(100) melting and solidification

U (kV)	A_1/A_2	$T_{s,\text{max}}$ (K)	t_0 (ns)	t_e (ns)	t_m (ns)	Z_{max} (nm)	$\left(\frac{dZ}{dt}\right)_{\text{max}}$ (ms^{-1})	$\left(\frac{dZ}{dt}\right)_{\text{min}}$ (ms^{-1})
24	3.97	1750	26.6	69.6	43.0	44.5	3.95	-2.46
22	3.70	1742	27.0	70.2	42.8	40.6	3.43	-2.35
21	4.84	1792	24.4	74.8	50.4	67.3	6.62	-3.05
20	6.13	1787	22.5	75.8	53.3	70.2	5.88	-3.41
19	11.2	1805	22.4	77.3	54.9	86.6	6.68	-4.61
18	10.0	1822	21.8	77.0	55.2	93.3	7.64	-4.72
16	10.9	1818	20.8	76.1	55.3	93.8	7.30	-4.74
-	triangle	1910	20.7	76.6	55.9	144.8	11.0	-5.87
-	trapezoid	1905	20.2	76.0	55.8	140.8	9.61	-5.87

the following characteristic parameters were compared: the maximum surface temperature, $T_{s,max}$, the time of melting onset, t_0 , the time of melting end, t_e , the melt duration, $t_m = t_e - t_0$, the maximum thickness of the molten layer, Z_{max} , and the maximum and minimum velocities of the solid/liquid interface, $(dZ/dt)_{max}$, $(dZ/dt)_{min}$. For all these computations, we used the value of energy density $E = \int I_0(t) dt = 1.0 \text{ J cm}^{-2}$.

Numerical results summarized in Table 2 exhibit the qualitative behaviour reflecting the three groups of pulse shapes. Differences up to 52% in Z_{max} , 22% in t_m , 4% in $T_{s,max}$ show that variations in the ratio A_1/A_2 due to the applied voltage cannot be neglected in any practical application. Two basic shapes of the pulse have also been considered: triangular (26 ns FWHM) and trapezoidal (31 ns FWHM) often used in previous calculations [8–12] (see Table 2). While the melt durations t_m do not exhibit any significant differences ($< 1\%$) comparing the pulse with the highest ratio A_1/A_2 to the ideal triangular and trapezoidal shapes, the maximum melt depths Z_{max} differ about approximately 35%. A comparison of results for triangular and trapezoidal pulses shows marked differences (about 12%) in $(dZ/dt)_{max}$ only, the differences in all other characteristic parameters being less than 3%.

Time dependencies of the surface temperature T_s , solid/liquid interface velocity, (dZ/dt) , and solid/liquid interface position Z for the three groups of pulses represented by the different A_1/A_2 ratios along with the triangular and trapezoidal pulses are shown in Figs. 3–5. The decreasing ratio A_1/A_2 corresponding to the prolonged tail of the pulse causes a slower decrease of surface temperature in the region $t > 70$ ns, as shown in Fig. 3. Also, the $(dZ(t)/dt)$ curves are apparently affected by the length of the tail, the maximum values of (dZ/dt) being shifted further in the time axis (see Fig. 5). Both melting and solidification processes get a more equilibrium character.

Fig. 6 shows that a prolonged tail of the pulse which is characteristic for the lower ratios A_1/A_2 always results in a shorter melt duration t_m and a higher value of melting threshold E_t when compared to ideal pulse of the same energy density

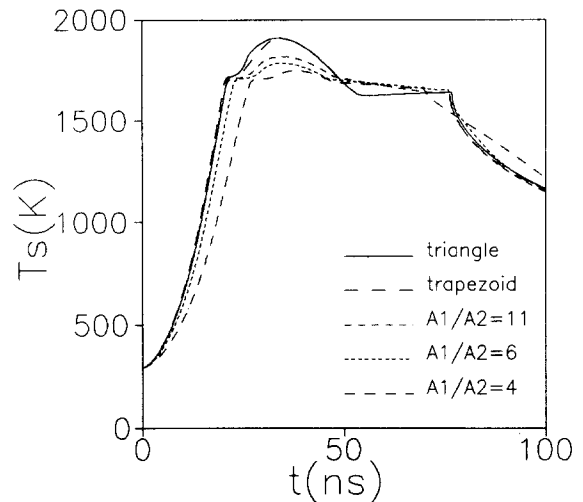


Fig. 3. Surface temperature for various temporal pulse shapes.

[e.g., the values of E_t for a triangular pulse ($A_1/A_2 \rightarrow \infty$) and for a “tailed” pulse with $A_1/A_2 = 4$ differ by approximately 25% and t_m up to 50%]. This is in a contradiction with theoretical calculations of Wood and Jellison [9] reporting that “melt duration is greatly prolonged by a long tail of the pulse”. The calculations were repeated using equilibrium thermal model of laser-induced melting and solidification (see Refs. [8,9], for details) which was used for the theoretic-

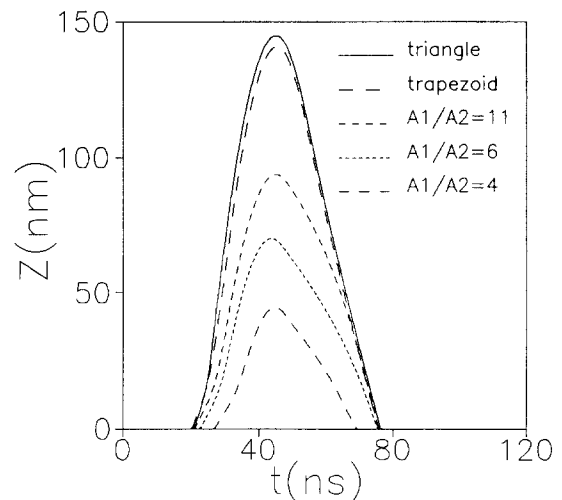


Fig. 4. Position of the solid/liquid interface for various temporal pulse shapes.

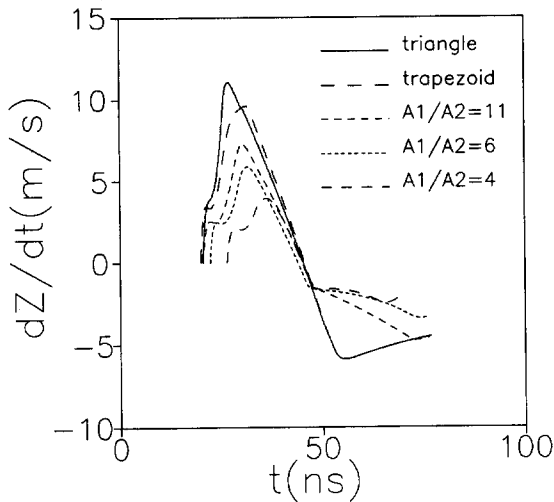


Fig. 5. Velocity of the solid/liquid interface for various temporal pulse shapes.

cal work in Ref. [9]. Differences up to 5% between the equilibrium and the nonequilibrium models have been found and there is nonsubstantial deviation in the course of $t_m = t_m(E)$. The contradiction between our results and the computational results from Ref. [9] cannot be simply

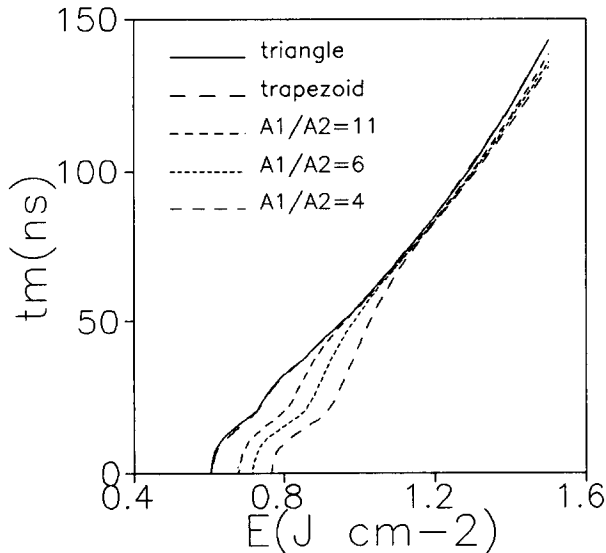


Fig. 6. Melt duration vs. energy density for various temporal pulse shapes.

explained by this way. Therefore, we can conclude that there might be some mistake in calculations by Wood and Jellison in Ref. [9].

5. Conclusions

To summarize our numerical simulations, the results show that the FWHM value is not a convenient parameter to characterize an excimer laser pulse. To obtain the correct thermodynamical parameters of irradiated surface from TRR curves by matching the experimental data with the theoretical model, which is the only reliable method (see Refs. [11,12]), it is necessary to consider the detailed time structure of the energy distribution in the laser pulse.

6. Acknowledgement

This paper is based upon work supported by Grant Agency of the Czech Republic, under grant No. 202/93/2383.

7. References

- [1] D.H. Auston, J.A. Golovchenko, A.L. Simons, C.M. Surko and T.N.C. Venkatesan, *Appl. Phys. Lett.* 34 (1979) 777.
- [2] J. Narayan and C.W. White, *Appl. Phys. Lett.* 44 (1984) 35.
- [3] G. Gorodetsky, J. Kanicki, T. Kazyaka and R.L. Melcher, *Appl. Phys. Lett.* 46 (1985) 547.
- [4] G.B. Shinn, F. Steigerwald, H. Stiegler, R. Sauerbrey, F.K. Tittel and W.L. Wilson Jr., *J. Vac. Sci. Technol. B* 4 (1986) 1273.
- [5] D.H. Lowndes, G.E. Jellison, Jr., S.J. Pennycook, S.P. Withrow and D.N. Mashburn, *Appl. Phys. Lett.* 48 (1986) 1389.
- [6] D.H. Lowndes, *Phys. Rev. Lett.* 48 (1986) 267.
- [7] D.H. Lowndes and G.E. Jellison Jr., in: *Pulsed Laser Processing of Semiconductors*, chap. 6, ed. R.F. Wood, C.W. White and R.T. Young (Academic, Orlando 1984).
- [8] R.F. Wood and G.E. Giles, *Phys. Rev. B* 23 (1981) 2923.
- [9] R.F. Wood and G.E. Jellison Jr., in: *Pulsed Laser Processing of Semiconductors*, chap. 4, eds. R.F. Wood, C.W. White and R.T. Young (Academic, Orlando, 1984).
- [10] S. de Unamuno and E. Fogarassy, *Appl. Surf. Sci.* 36 (1989) 1.
- [11] R. Černý, R. Šášik, I. Lukeš and V. Cháb, *Phys. Rev. B* 44 (1991) 4097.

- [12] I. Lukeš, R. Šášik and R. Černý, *Appl. Phys. A* 54 (1992) 327.
- [13] G.E. Jellison, Jr., D.H. Lowndes, D.N. Mashburn and R.F. Wood, *Phys. Rev. B* 34 (1986) 2407.
- [14] R.F. Wood and G.A. Geist, *Phys. Rev. B* 34 (1986) 2606.
- [15] Numerical Data and Functional Relationships in Science and Technology, Landolt-Boernstein New Series, vol. 17 (Springer, Berlin, 1982).
- [16] C. Kittel, *Introduction to Solid State Physics* (Wiley, New York, 1976).
- [17] M.D. Kluge and J.R. Ray, *Phys. Rev. B* 39 (1989) 1738.